Colloid Polym Sci (2004) 283: 344–350
DOI 10.1007/s00396-004-1143-y

ORIGINAL CONTRIBUTION

Fadhel Aloulou
Sami Boufi
Naceur Belgacem
Alessandro Gandini

Adsorption of cationic surfactants and subsequent adsolubilization of organic compounds onto cellulose fibers

Received: 13 February 2004
Accepted: 27 April 2004
Published online: 4 June 2004

F. Aloulou · S. Boufi
LMSE, Faculté des sciences de Sfax,
BP 802 3018 Sfax, Tunisia

N. Belgacem (✉) · A. Gandini
LGP2, Ecole Française de Papeterie et des Industries Graphiques (INPG),
BP 65, 38402 St. Martin d'Hères,
France
E-mail: naceur.belgacem@efpg.inpg.fr
Tel.: +33-4-76826962
Fax: +33-4-76826933

Abstract Cationic surfactants with different hydrophobic chain length were adsorbed onto cellulose fibers in an aqueous medium. The adsorption isotherms exhibited three characteristic regions which were interpreted in terms of the mode of aggregation of the surfactant molecules at the solid–liquid interface. The hydrophobic layers were used as a reservoir to trap various slightly water soluble organic molecules. A quantitative study of these phenomena suggested typical partition behavior of the organic solutes between the aqueous phase and the surfactant layer. The surfactant chain length (from C12 to C18) was shown to play an important role in terms of the capacity to retain the organic solute and the capacity increased with the number of carbon atoms.

Keywords Cellulose fibres · Adsolubilisation · Cationic surfactants · Organic pollutants removal

Introduction

Surfactant adsorption at the solid–liquid interface is a phenomenon of significant importance for many industrial processes, such as selective flotation [1], cosmetic formulation, paint technology, and ceramic processing. The study of the adsorption of ionic surfactants on charged surfaces has led to the concept of aggregation and self-assembly of the surfactant at the solid–liquid interface [2, 3, 4, 5, 6]. Three models for the adsorbed layer structure have been proposed. The reverse orientation model, first proposed by Somasundaran and Fuerstenau [7, 8], is based on a sequence of four steps for the surfactant adsorption. The first involves the individual surfactant adsorption via an ion-exchange mechanism exclusively; in the second step, the aggregation into hemimicelles takes place as a result of the reorganization, accompanied by an association process, which led to the formation of a surfactant monolayer oriented with the head groups in contact with the solid surface; the third step considers the increase of the density of the aggregated domains through further surfactant adsorption; finally, the fourth step involves the formation of bilayer-organized structures which saturate the surface. The second model, proposed by Harwell et al. [9], differs slightly from the previous one, in that patches of bilayer structures, termed admicelles, are formed as soon as the concentration of free surfactant attains a critical level, without hemimicelle formation at lower surfactant concentrations. A different model was proposed by Gu and coworkers [10, 11], according to which the surfactant adsorption proceeds through two phases: the first results from electrostatic interactions between the surfactant head groups and the surface charges and the second involves lateral interactions among the alkyl chains which induce the formation of a bundle of adsorbed surface micelles that become progressively more closely packed as further surfactant is adsorbed.

In all of these models, the adsorption process is a result of two mechanisms. First, the electrostatic interaction between the surface and the ionic surfactant head groups give rise to an adsorption characterized by the lack of any particular configuration of the surfactant molecules at the solid–liquid interface. Subsequently, following the attainment of a critical concentration, lateral hydrophobic interactions among the hydrocarbon chains bring about the reorganization and the aggregation of the adsorbed surfactant molecules at the substrate surface. The driving force for this association process is the reduction in contact area between the hydrocarbon lyophobic tails and the surrounding water molecules, which gives rise to an increase in the configurational entropy.

Many experimental techniques, such as zeta potential [5, 12] and contact angle measurements [13], fluorescence intensity [4, 14], Fourier transform IR spectroscopy [15] and electron spin resonance [16, 17], have been used to study the aggregation of surfactant molecules at the solid–liquid interface. Only recently the use of atomic force microscopy has provided clear-cut evidence of self-assembly by direct imaging of the interface [18, 19].

The aggregation of surfactant molecules at the solid–liquid interface generates hydrophobic cores formed by the associated surfactant tails on which organic compounds can be trapped. This process, termed adsolubilization, stimulated much research and has found many applications in different domains, such as surface modification using admicellar polymerization [20, 21], chromatographic separation [22], wastewater treatment [23, 24, 25, 26] and drug carrier targeting in pharmacology [27]. However, to the best of our knowledge, all these studies concentrated on the adsolubilization behavior of inorganic oxides [25, 26, 27, 28, 29, 30, 31, 32], particularly SiO_2, Al_2O_3 and TiO_2. Much effort has been devoted to understand the different mechanisms involved in the adsolubilization process using these substrates, by investigating the effect of various parameters, such as the medium pH [32], the ionic strength [33], and the surfactant [34] and solute structures [35]. Among the drawbacks related to inorganic oxides, one finds their vulnerability to the medium characteristics (pH, ionic strength) and the requirement of extremely fine particles in order to attain surface areas high enough for appreciable surfactant uptake.

In this work, we pursue our investigation on the interactions of surfactants with a poorly charged organic substrate [21, 36], namely cellulose fibers and the aptitude of these treated substrates to trap organic compounds in aqueous media. Our interest in cellulose fibers was motivated by the abundance of this natural polymer, its worldwide availability at a low cost and in numerous varieties and its biorenewable character. The surface properties of cellulose fibres at the solid–liquid interface were first investigated by de Groot and Dékany [37].

Experimental

Materials

The fibers used in this work were a commercial TECHNOCEL-150DM sample of microcrystalline cellulose. Their average length was about 250 μm and their specific surface, measured by the Brunauer–Emmett–Teller technique using nitrogen as the probe was found to be 2.5 $m^2\ g^{-1}$. The presence of negative surface charges was confirmed by zeta potential measurements which gave an average value of −10 mV at pH 6.5–7 and ionic strength of 10^{-3}. Conductivity measurements provided a value of about 55 μmol of negative charges per gram.

Four commercial analytical grade cationic surfactants were used, namely octadecyltrimethylammonium bromide (C18), hexadecylpyridinium chloride (C16), tetradecyltrimethylammonium bromide (C14) and dodecylpyridinium chloride (C12). Their critical micelle concentrations (cmcs) at 25 °C are 2.1×10^{-4}, 7.5×10^{-4}, 3.4×10^{-3} and 1.2×10^{-2} M, respectively.

All the organic solutes used in this study were of analytical grade commercial products.

Adsorption and adsolubilization isotherms

The adsorption isotherms related to the surfactants were obtained in the presence of 1 wt % cellulose dispersed in water. The suspensions were then stirred for 24 h at room temperature to reach adsorption equilibrium. The coadsorption of organic solutes was performed as follows. To equilibrated aqueous surfactant-cellulose suspensions, prepared as previously described, a known amount of the selected organic solute was added using a microsyringe for liquid solutes or by weighing the solid powder counterpart. The ensuing suspension was then shaken for 4 h at room temperature to reach the adsolubilization equilibrium.

The dispersions were then centrifuged at 2,500 rpm for 15 min. The supernatant concentrations of the organic solute and the surfactant were determined by UV spectroscopy and colorimetric titration, respectively. In the case of sparingly soluble solutes (solubility lower than 5×10^{-4} M), the adsolubilized amount was determined by UV spectroscopy after its extraction from the cellulose fibers with ethanol and the supernatant concentration was determined by the difference. The colorimetric titration of the cationic surfactant was performed using a starch solution and iodine. The principle of the method is based on the aptitude of ionic linear surfactants to form stable inclusion complexes with amylose [38]. The details of the procedure have already been described [36]. Both the UV and the colorimetric analyses were conducted on the basis of previously established calibration curves.

Results and discussion

Surfactant adsorption onto cellulose fibers

The adsorption isotherms of each cationic surfactant onto cellulose fibers are shown in Fig. 1a and b following two different modes of presentation, viz., linear–linear and linear–log plots, the latter being useful to amplify the low concentration range of the isotherms. In this figure the amount of surfactant adsorbed is plotted against the surfactant equilibrium concentration. The linear–linear plots display an initial steep rise followed by a smooth ascent towards an asymptotic value. The initial steep rise suggests a high affinity of the cationic surfactants towards the cellulose fiber surface. The plateau value, on the other hand, increases as the surfactant chain length increases. The linear–log representations clearly show sigmoidal behavior similar to that already observed for long-chain surfactants adsorbed on charged inorganic oxide surfaces [39]. The isotherms plotted in this way can be subdivided into three regions, following previous studies [32, 33, 34, 35, 39, 40], reflecting different modes of surfactant–surface interactions:

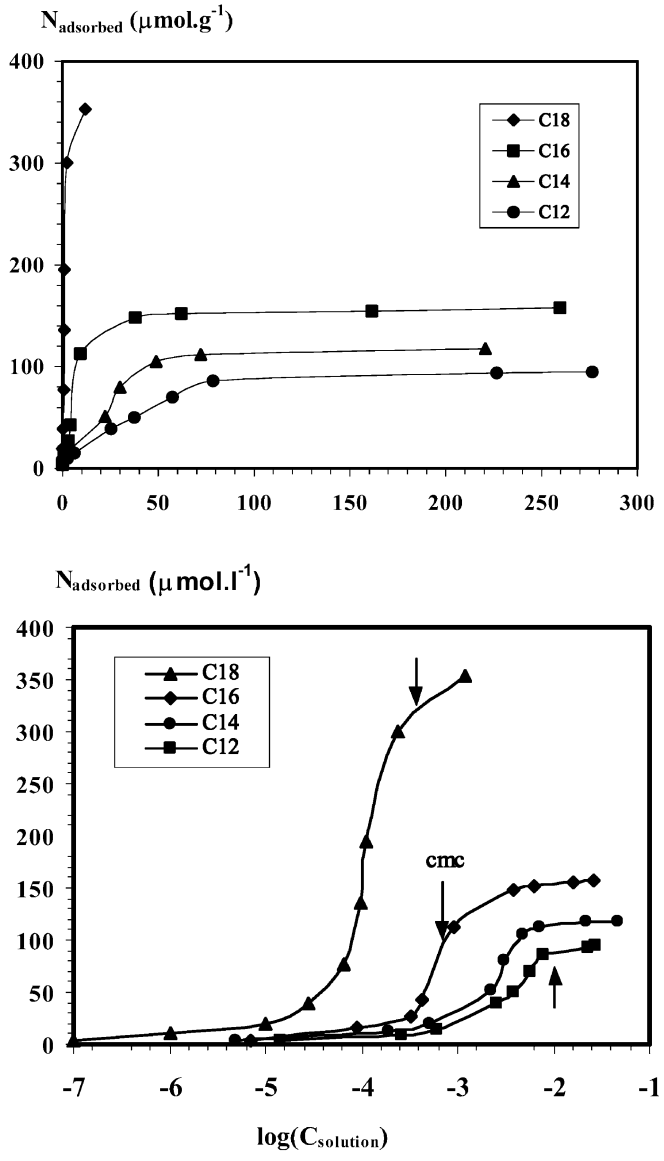

Fig. 1 Adsorption isotherms of cationic surfactants on cellulose fibers: **a** according to a linear–linear scale, **b** according to a linear–log scale

1. At low surfactant concentration, the amount adsorbed increases very slowly with increasing surfactant concentration; in this domain, adsorption occurs principally through electrostatic interactions between negative surface charges of cellulose (essentially carboxylic groups arising from certain hemicelluloses and/or oxidative bleaching of cellulose) and the positive ammonium surfactant head groups. The maximum amount of adsorbed surfactant in this region does not exceed 30 μmol g^{-1}, with this relatively low value probably being related to the low surface charge of cellulose of 50 μmol g^{-1}.
2. The second region starts with a sharp increase in the amount of the adsorbed surfactant, which indicates the onset of the lateral hydrophobic interactions among surfactant tails which gives rise to the aggregation of the surfactant molecules at the solid–liquid interface.
3. The third region is characterized by the approach to a saturation value in the amount of the surfactant adsorbed and therefore a major increase in the surfactant concentration does not lead to a corresponding change in the amount adsorbed. This behavior suggests that the packing density of the surfactant molecules on the cellulose surface is such that the lateral electrostatic repulsion between the charged head groups balances the attractive hydrophobic interactions of adjacent hydrocarbon tails. The onset of this region appears to be close to the cmc of the corresponding surfactants as indicated by the arrows in Fig. 1b.

An increase in the alkyl chain length led to an increase of both the slope of region 2 and the plateau level. These trends are in agreement with the aggregation hypothesis of the adsorbed surfactant molecules. Indeed, the addition of CH_2 groups to the surfactant tail enhances the extent of hydrophobic interactions among alkyl chains, thereby increasing the adsorption, just as in the well-known correlation between the increase in the surfactant chain length and the corresponding decrease of its cmc.

Even though the surface charge density of the cellulose fibers is much lower than that of typical inorganic oxides, the adsorption behavior of the surfactants

appears to take place in a similar manner at both surfaces. This fact highlights the predominant role of the hydrophobic interactions among the surfactant tails in the adsorption process. The adsorption mechanism is likely to be entropy-driven, since when surfactant molecules associate themselves at the substrate surface, the water molecules surrounding the hydrocarbon tails are released into the bulk aqueous medium, thus increasing the entropy of the system.

In spite of the low surface area measured for the cellulose fibers used in this study (2.5 $m^2\ g^{-1}$), the maximum amounts of surfactants adsorbed were relatively high, considering that other substrates display such adsorption levels only with specific surface areas higher than 150 $m^2\ g^{-1}$[30, 31, 41]. This apparent discrepancy can be rationalized by assuming that the surfactant molecules were adsorbed not only at the external surface of the fibers, but could also diffuse inside their porous structures thanks to their swelling in the aqueous medium. In other words, the actual cellulose surface available for surfactant adsorption in the aqueous swollen state was much larger than that measured on the dry substrate. Assuming that the adsorbed surfactant molecules were oriented perpendicularly to the cellulose substrate and 65 A^2 [42] is taken as the surface covered by the trimethylammonium group, the specific surface area of the swollen cellulose substrate was estimated to be about 110 $m^2\ g^{-1}$, which is more than 40 times the corresponding value for the dry material.

The effect of the medium pH and ionic strength on the adsorption isotherm was studied using the C16 surfactant. Figure 2 shows that, regions 1 and 2 were little affected by the pH modification, whereas the plateau value of region 3 increased by a factor 1.5 as the pH was raised from 3 to 10. Since the carboxylic groups are fully ionized up to a pH value of 5–5.5, we attribute the latter effect to the well-known swelling of the cellulose matrix induced by the rise in pH which led to an increase in the available solid–liquid interface [43].

The effect of the ionic strength on the adsorption isotherm is shown in Fig. 3. Again, the basic qualitative features related to regions 1 and 2 were not drastically modified and again a significant quantitative change occurred, with regard to the plateau value, which increased as the electrolyte concentration was increased. This behavior is most probably related to a growing screening effect of electrolyte ions inducing a corresponding decrease in electrostatic repulsion among the charged head groups of the adsorbed surfactant. The net effect of this phenomenon was therefore a progressive increase of the surfactant surface density as the ionic strength increased.

Figure 4 displays the adsorption kinetics related to the four surfactants. The time needed to attain equilibrium was found to be inversely related to the length of the hydrophobic chain, namely, about 20, 17, 15 and 7 h for C12, C14, C16 and C18, respectively. In the case of C12, an induction period of about 5 h occurred before the slow adsorption feature. On the whole, these adsorption times are particularly long, but are consistent with a mechanism based on the slow diffusion of the surfactant molecules inside the cellulose fibers. The inverse trend can be rationalized by the fact that the longer the hydrophobic chains are, the easier it is to overcome

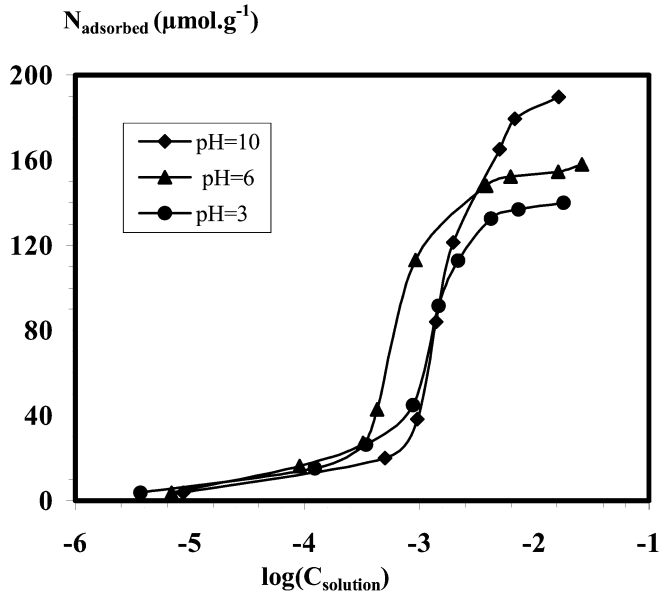

Fig. 2 Adsorption isotherms of the C16 surfactant on cellulose fibers at three different pH values

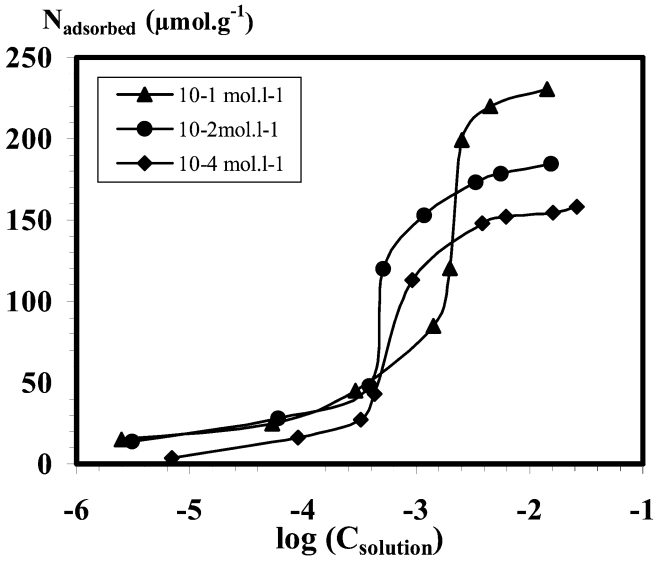

Fig. 3 Adsorption isotherms of the C16 surfactant at pH 6.7–7 and three different ionic strengths (addition of KCl)

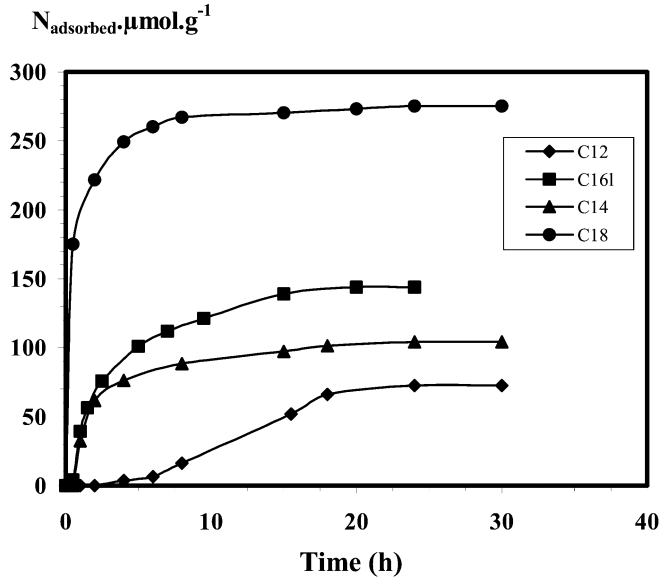

Fig. 4 Time evolution of the amounts of the different cationic surfactants adsorbed on cellulose fibers at a constant surfactant concentration of 10^{-3} M

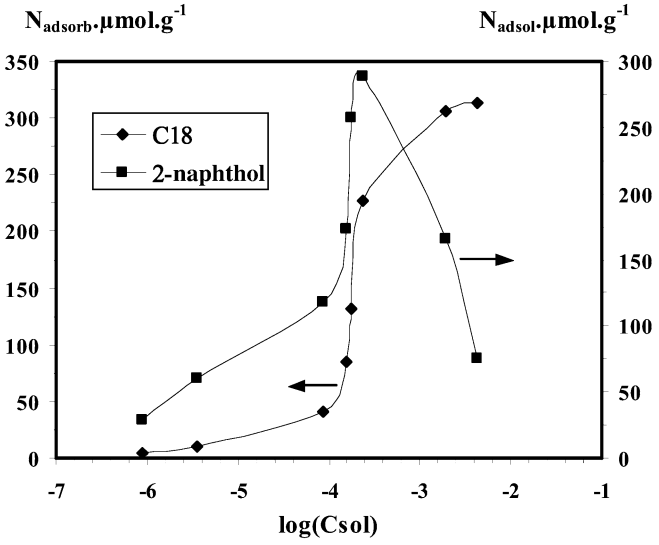

Fig. 5 *C18*adsorption isotherm and *2-Naphthol*adsolubilization isotherm as a function of the equilibrium C18 concentration at pH 6.5–7

the capillary pressure inside the fiber micro pores and thus hasten the diffusion process of the surfactant molecules.

Adsolubilization behavior of organic solutes

The second part of our study concerned the effect of the surfactant adsorption on the adsolubilization behavior of the cellulose fibers. The relationship between the equilibrium C18 adsorbed surfactant concentration and the corresponding amount of 2-Naphthol coadsorbed is shown in Fig. 5. The comparison of these two isotherms clearly indicated a progressive 2-Naphthol adsolubilization accompanying the corresponding increase of C18 adsorption, up to a sharp critical value, after which the extent of 2-Naphthol retention decreased dramatically. This drastic downturn occurred at a C18 surfactant concentration very close to its cmc. The increase in adsolubilization at surfactant concentrations below the cmc clearly suggests that the formation of admicellar structures around the fibers constitutes an efficient reservoir for the added organic compound (it is important to emphasize that 2-Naphthol was adsorbed onto the cellulose fibers in negligible amounts in the absence of surfactant). This hypothesis was corroborated by the observation that the C18 adsorption isotherm did not change significantly in the presence of the organic compound, which indicated that the latter was indeed adsolubilized inside the aggregated surfactant domains.

The coincidence of the occurrence of the sharp downturn and the C18 cmc strongly suggests that once free micelles began to form in the aqueous solution, 2-Naphthol could distribute itself between the adsorbed layer and the bulk micelles, which led to a progressive decrease of its presence in the former (as clearly shown in Fig. 5) as the concentration of the latter increased.

Several other organic compounds were tested in this context and the results obtained, again using C18, are shown in Fig. 6. A common trend was observed, irrespective of the specific structure of the molecules added, confirming that they were indeed adsolubilized within the hydrophobic adsorbed surfactant layer, rather than fixed by structure-specific interactions with the surfactant head groups.

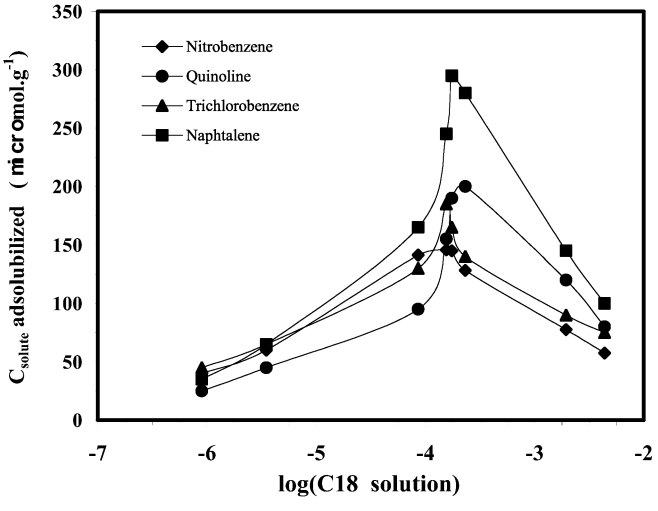

Fig. 6 Adsolubilization isotherms of different organic compounds as a function of the equilibrium C18 concentration at pH 6.5–7

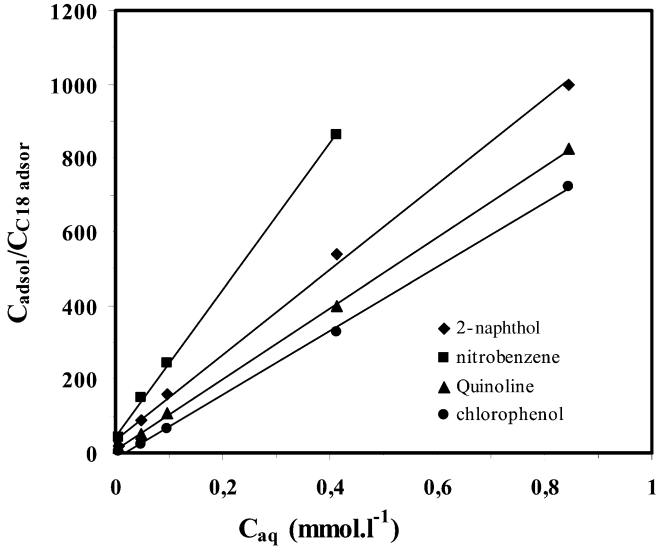

Fig. 7 Adsolubilized solute fraction versus its equilibrium concentration

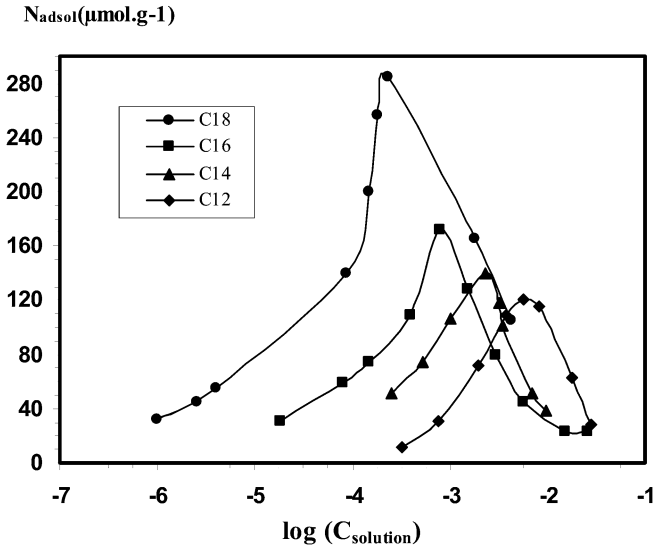

Fig. 8 Adsolubilization isotherms of 2-Naphthol onto cellulose fibers as a function of the surfactant alkyl chain length

In the same way as for the solubilization process in the presence of free surfactant micelles, the adsolubilization phenomenon can be viewed as the partition of the organic compound between the hydrophobic core of the adsorbed surfactant layer and the aqueous phase.

It follows that the partition coefficient can be defined as the ratio between the mole fraction of solute in the adsorbed surfactant layer (X_{adsol}) and the solute concentration in the aqueous phase (C_{aq}):

$$K_{ads} = \frac{X_{adsol}}{C_{aq}},$$

where $X_{adsol} = C_{adsol}/C_{surf\ adsor}$.

Convincing evidence for the validity of this partition approach was obtained thanks to the linear behavior of the corresponding plots of all the organic solutes tested, four of which are shown in Fig. 7. The relevant partition coefficient data are provided in Table 1. The relatively high values obtained indicate that the cellulose fibers treated with C18 possessed a high affinity towards organic compounds. It is interesting to note that both the partition coefficient and the maximum adsorbed concentration seemed to depend on the extent of the polar character of the molecular structure in the sense that the lower this contribution, the higher the amount that was adsolubilized, as shown in Table 1.

The effect of the surfactant chain length on the adsolubilization capacity was studied using 2-Naphthol. The adsorption isotherms of this compound in the presence of each of the four surfactants are shown in Fig. 8, and the corresponding quantitative parameters are given in Table 2.

Table 1 Results related to the adsolubilization of different organic compounds on C18-treated cellulose fibers

Organic solute	K_{adsol}	$C_{max\ adsol}$ (µmol l^{-1})
Benzene	8,900	390
Cholrobenzene	6,450	310
1,3,5-Tricholorobenzene	5,000	185
Nitrobenzene	1,920	194
2-Naphthol	1,960	290
Naphtalene	6,750	304
2-Cholorophenol	980	169
Quinoline	1,050	202

Table 2 Results related to the adsolubilization of 2-Naphthol as a function of the surfactant alkyl chain length

Surfactant	K_{adsol}	$C_{max\ adsol}$ (µmol l^{-1})
C18	1,963	295
C16	1,310	180
C14	928	140
C12	730	120

The features of the four curves were qualitatively the same but followed quantitatively two clear-cut trends, viz., (1) a decrease in the maximum amount adsorbed with decreasing hydrophobic chain length, and (2) a shift in the position of that maximum related to the corresponding surfactant cmc. The first trend gave rise to the changes in the partition coefficient shown in Table 2 and suggested that the increase in the surfactant chain length, which gives rise to a larger hydrophobic volume of the adsorbed layer, provided a correspondingly higher capacity of storage of the organic molecules.

Conclusion

Surfactant-modified cellulose fibers appeared to be effective sorbents for the removal of organic compounds dissolved in aqueous media. Given the ready availability of this type of substrate and its low cost, the present approach could be promising in applications related to the removal of organic pollutants and toxic substances in wastewaters. However, the possible desorption of the surfactant molecules from the cellulose surface should be impeded, for example, by their chemical coupling through covalent bonding. Work is in progress to study this possibility.

Acknowledgements This work was supported by the International Foundation for Science through grant W/3358-1. We also wish to thank the Tunisian "Secrétariat d'Etat à la Recherche Scientifique et Technologique" for its financial support.

References

1. Frommer DW (1967) J Am Oil Chem Soc 44:270–274
2. Clunie JS, Ingram BT (1983) In: Parfitt CD, Rochester CH (eds) Adsorption from solution at the solid/liquid interface. Academic, New York, p 105
3. Scamehorn JF, Schechter RS, Wade WH (1982) J Colloid Interface Sci 85:463–478
4. Chandar P, Somasundaran P, Turro NJ (1987) J Colloid Interface Sci 117:31–46
5. Fuerstenau DW (1956) J Phys Chem 60:981–985
6. Clint JH (1992) Surfactant aggregation. Chapman and Hall, New York, chap 9
7. Somasundaran P, Fuerstenau DW (1996) J Phys Chem 70:90–96
8. Somasundaran P, Fuerstenau DW (1972) Trans AIME 252:275–279
9. Harwell JH, Hoskins JC, Schechter RS, Wade WH (1985) Langmuir 1:251–262
10. Gu T, Huang Z (1989) Colloids Surf 40:71–76
11. Rupprecht H, Gu T (1991) Colloid Polym Sci 269:506–522
12. Lin IJ, Somansundaran P (1971) J Colloid Interface Sci 37:731–743
13. Singh PK, Adler JJ, Rabinovich YI, Moudgil BM (2001) Langmuir 17:468–473
14. Esumi K, Sakamoto Y, Meguro K (1989) Colloid Polym Sci 267:525–530
15. Sperline RP, Song Y, Freiser H (1997) Langmuir 13:3727–3732
16. Waterman KC, Turro NJ, Chandar P, Somasundaran PJ (1986) Phys Chem 90:6828–6830
17. Esumi K, Otsuka H, Meguro K (1990) J Colloid Interface Sci 136:224–230
18. Patrick HN, Warr GG, Manne S, Aksay IA (1999) Langmuir 15:1685–1692
19. Kovacs L, Warr GG (2002) Langmuir 18:4790–4794
20. Wu J, Harwell JH, O'Rear EA (1987) Langmuir 3:531–537
21. Boufi S, Gandini A (2001) Cellulose 8:303–312
22. Barton JW, Fitzgerald TP, Lee C, O'Rear EA, Harwell JH (1988) Sep Sci Technol 23:451–474
23. Boyd SA, Lee JF, Mortland MM (1988) Nature 333:345–347
24. Lee JF, Grum J, Boyd SA (1989) Environ Sci Technol 23:1365–1372
25. Burris DR, Antworth CP (1992) J Contam Hydrol 10:325–337
26. Nayyar SP, Sabatini DA, Harwell JH (1994) Environ Sci Technol 28:1874–1881
27. Hayakawa K, Mouri Y, Maeda T, Satake I, Sato M (2000) Colloid Polym Sci 278:553–558
28. Esumi K, Matoba M, Yamanaka Y (1996) Langmuir 12:2130–2135
29. Esumi K, Maedomari N, Torigoe K (2000) Langmuir 16:9217–9220
30. Monticone V, Treiner C (1994) J Colloid Interface Sci 166:394–403
31. Dickson J, O'Haver J (2002) Langmuir 18:9171–9176
32. Esumi K, Toyoda H, Goino M, Suhara T, Fukui H (1998) Langmuir 14:199–203
33. Esumi K, Goino M, Koide Y (1996) Colloids Surf 118:161–166
34. Esumi K, Goino M, Koide Y (1996) J Colloid Interface Sci 183:539–545
35. Zhu L, Ren X, Yu S (1998) Environ Sci Technol 32:3374–3378
36. Aloulou F, Boufi S, Chakchouk M (2004) Colloid Polym Sci 282:699–713
37. De Groot J, Dékany I (1992) Colloid Polym Sci 270:470–477
38. Godet MC, Buleon A., Tran V, Colonna P (1993) Carbohydr Polym 21:91–95
39. Gouloub T, Koopal LK (1997) Langmuir 13:673–681
40. Monticone V, Treiner C (1995) Colloids Surf 104:285–293
41. Thakulsukaant C, Lobban LL, Osuwan S, Waritswat A (1997) Langmuir 13:4595–4599
42. Rosen MJ (1989) Surfactant and interfacial phenomena. 2nd edn. Wiley-Interscience, New York
43. Zernian SH (1985) In: Nevell TP, Zeronian SH (eds) Cellulose chemistry and its applications. Harwood, Chichester, pp 141–165